OPTICAL DESIGN OF SUB-MILLIMETER SPECTROMETER FOR LIMB SOUNDER

P. Yagoubov[1], H. van de Stadt[1], R. Hoogeveen[1], V. Koshelets[1,2], M. Birk[3], A. Murk[4]

[1]*National Institute for Space Research, SRON, Landleven 12, 9747 AD Groningen, the Netherlands*
Email: p.a.yagoubov@sron.rug.nl

[2] *Institute of Radio Engineering and Electronics (IREE), Mokhovaya 11, Bldg. 7, Moscow125009, Russia*
Email: valery@hitech.cplire.ru

[3]*Institute for Remote Sensing Technology, DLR, Muenchner Str. 20, D-82234 Wessling, Germany*
Email: manfred.birk@dlr.de

[4]*Institute of Applied Physics, University of Bern, Sidlerstr. 5, CH-3012 Bern, Switzerland*
Email: axel.murk@mw.iap.unibe.ch

ABSTRACT

TELIS (Terahertz and submm Limb Sounder) is a cooperation between DLR (Institute for Remote Sensing Technology, Germany), RAL (Rutherford Appleton Laboratories, UK) and SRON (National Institute for Space Research, the Netherlands), to build a three-channel balloon-borne heterodyne spectrometer for atmospheric research. The three receivers will operate simultaneously at 500 GHz (channel developed by RAL), at 550-650 GHz (SRON in collaboration with IREE), and at 1.8 THz (DLR). The balloon platform on which TELIS will fly also contains a Fourier transform spectrometer: MIPAS-B developed by the IMK (Institute of Meteorology and Climate research of the University of Karlsruhe, Germany). MIPAS-B will simultaneously measure within the range 680 to 2400 cm^{-1}. The combination of the TELIS and MIPAS instruments will provide an unprecedented wealth of scientific data and will also be used to validate other instruments and atmospheric chemistry models. In this paper we present the optical design of TELIS with an emphasis on the 550-650 GHz channel. The main design goal was to generate a high efficiency antenna beam over the full frequency range, with low side lobes and close to diffraction limited angular resolution in the vertical direction at the sky. All these requirements had to be achieved within a small volume and low mass. Design and validation of the optics, as well as estimation of optical components tolerances, was done using commercial software packages ZEMAX and GRASP.

1 TELESCOPE AND WARM OPTICS

The optical front-end of TELIS (Terahertz and submm Limb Sounder) instrument consists of a pointing telescope, calibration blackbody and relay optics, common for the three channels: 500 GHz, 550-650 GHz and 1.8 THz [1].

The telescope is a dual offset Cassegrain antenna. Primary, secondary and tertiary mirrors of the telescope are mounted on a common frame. The unit is rotated as a whole around the axis coinciding with the direction of the output beam to scan the beam through the required limb sequence on the sky. Primary parabola has an elliptical cross-section of 260x140 mm. 2:1 anamorphicity is introduced by the cylindrical tertiary mirror, which is flat in the vertical direction and spherical in horizontal. An anamorphic design was selected to improve telescope compactness, mass, and moment of inertia. A vertical (elevation) resolution at the tangent point is about 2 km at 500 GHz (FWHM), inversely proportional to the frequency. The limb scans range from upper troposphere (10 km) to stratosphere (30-40 km). Horizontal (azimuth) resolution is about a factor of 2 worse but not of prime importance for this mission as the atmospheric properties within the beam depend only on the altitude.

Calibration of the radiometric gain of the spectrometers is done with two blackbody reference sources at submillimeter wavelengths: the hot-load, which is a conical black-body at the ambient temperature, and the cold sky. The two references are measured in every antenna scan. The cold sky reference is measured with the telescope set at 40 degree upwards with respect to the limb position. For the hot load calibration, a switching mirror is inserted between the telescope and the warm optics for the TELIS receivers to view the reference.

Frequency separation between the channels is performed quasioptically, allowing simultaneous observations of all receivers. First, one linear polarization of the incoming signal is selected by a wire grid and is reflected into the 500 GHz channel. The other linear polarization, which is transmitted by the grid, is then split between two other frequency channels by a dichroic filter. After the splitting, the three beams enter a liquid helium cooled cryostat, where each receiver has dedicated cold optics and mixer elements. A number of off-set reflectors are used to interface the optics from the telescope to the cryogenic channels.

Detailed description of the telescope & warm optics is beyond the scope of this paper and is reported elsewhere [2]. Fig. 1 shows only schematics of the optics directly related to the 550-650 GHz channel. The optical beams of the two other frequency channels after the splitting as well as their dedicated optical elements are not shown here.

2 550-650 GHZ COLD CHANNEL DESIGN

The 550-650 GHz channel of the TELIS instrument is based on a phase-locked Superconducting Integrated Receiver (SIR) [3,4]. SIR is an on-chip combination of a low-noise SIS mixer with quasioptical planar antenna, a superconducting Flux Flow Oscillator (FFO) acting as Local Oscillator (LO) and SIS Harmonic Mixer (HM) for FFO phase locking, Fig. 2. The microcircuit is designed as a complete quasioptical heterodyne detection system. Physical size of the chip is 4x4 mm^2.

2.1 Integrated lens-antenna

The SIR chip is placed on the flat back surface of a Si lens, forming an integrated lens-antenna system, Fig. 3. The extra lens is needed to increase directivity, as the beam produced by a planar feed antenna itself (double-dipole or double-slot antennas are used) is inherently very wide. If radiated into the infinite dielectric with a relative dielectric constant of ε_r=11.7, the -10 dB beamwidth of such antennas is about 50º. The radiation properties of the integrated lens-antenna are in general determined by the properties of both the planar antenna and the lens, as well as the extension length of the lens [5]. In particular, as the extension length increases, the directivity increases until it reaches a maximum diffraction-limited value, determined by the diameter of the lens. While the directivity increases at higher extension length, the coupling to a fundamental

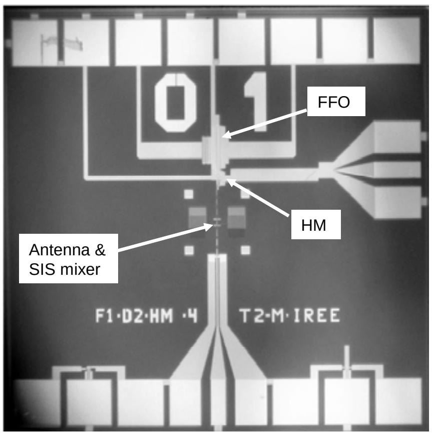

Fig. 2. Photo of the SIR chip. Double-slot antenna coupled SIS mixer, FFO and HM are located on a 4x4 mm^2 chip.

Gaussian beam decreases due to increased aberrations introduced by the lens and reflection loss at the lens surface. One of the constraints implied by SIR is a requirement to position the receiver chip inside a cylindrical magnetic shield, because the FFO is very sensitive for external magnetic interference. The cylinder is 90 mm long and has an inner clear aperture of 25 mm. Thus the integrated lens-antenna configuration should be compatible with large f-number optics. This is realized by using an elliptical lens and locating the feed antenna at the more distant focus of the ellipse. The lens diameter of 10 mm is selected by optimizing for the minimum beam size at 100 mm from the integrated lens-antenna at 550-650 GHz, so that the shielding cylinder does not truncate the beam. To minimize the reflection loss at the lens-air interface, the curved surface of the lens is coated with a 74 micron thick Stycast antireflection coating, optimized for the center frequency 600 GHz.

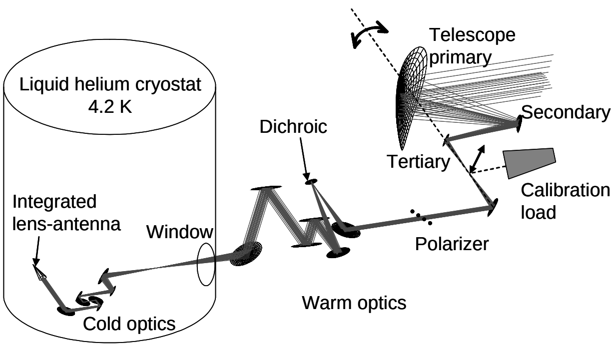

Fig. 1. Schematics of the 550 650 GHz channel optics. The telescope is rotated around the axis coinciding with the direction of the output beam. Wire grid polarizer and dichroic plate are used to separate this receiver from the two other frequency channels (not shown). The cold optics and mixer element are located inside the cryostat at the ambient temperature 4.2 K.

Fig. 3. Schematic drawing of the integrated lens-antenna. The SIR chip is glued to the back side of the elliptical silicon lens. Curved surface of the lens is coated with Stycast to minimize reflections at the silicon-air interface.

The quasi-optical performance of the lens-antenna system has been analysed with the ESA program PILRAP (Program for Integrated Lens and Reflector Antenna Parameters). PILRAP computes the beam patterns of the lens-antenna system by using Geometrical Optics to calculate the fields inside the lens (and thus, the fields at the lens surface). Angle- and polarization-dependent Fresnel reflection at the lens-coating-air interface is taken into account, as is radiation lost to the rear lobe of the antenna, and truncation of the antenna beam by the lens extension. Physical Optics is used to calculate the near- and far-field antenna patterns outside the lens. Table 1 summarizes main parameters of the integrated lens-antenna calculated at 625 GHz. The calculated spillover loss includes the power lost to the rear lobe of the planar feed antenna, 9% in case of double-slot antenna.

2.2 Cold channel configuration

The SIR cold channel optics consists of the integrated lens-antenna, Martin-Puplett polarizing interferometer used as a SSB (Single Side Band) filter and a number of curved and fold mirrors, all located in the liquid helium cryostat at the ambient temperature 4.2 K. The layout of the optics is shown in the Fig. 4. The SSB separates the optical frequency bands of the mixer above and below the LO frequency into two orthogonally polarized beams [6,7]. These two polarizations are then split by a wire grid. One polarization (and thus one sideband of the mixer) is transmitted through to detect the sky signal. The other polarization due to the other mixer sideband is reflected by the grid and thus terminated at a cold (4.2 K) load, or image load. Tuning of the SSB structure is done by moving one of the reflecting roof mirrors. This tuning mechanism uses flex pivots for the movement and an electromagnetic coil as driving motor.

The interface of the SIR channel optics to the telescope & warm optics system is defined at the position of an image of the pupil which is located outside the cryostat window 160 mm in front of the warm parabolic mirror. The interface accepts a "parallel" and frequency independent beam. The input beam waist has a radius of 11.0 mm for all frequencies. An off-axis parabolic mirror (L1) focuses the beam into an image of the sky located about 70 mm behind the cryostat window (L2). Note that the off-axis angles towards the focus of the parabola are not equal, they differ by as much as 10%. As a consequence, the focal spot will also be asymmetric. Between the mirror (L1) and the first cold mirror (L3) the cryostat window (L2), infrared radiation filter (not shown in the Fig. 4) and a grid for injecting the cold image load are located. The ellipse L3 serves as an optical relay. Just in front of the shielding cylinder is a combination of 2 curved mirrors (L4 and L5). With suitable focal lengths they image the system-pupil in the front surface of the integrated lens antenna. Thus we have frequency independent imaging. A de-magnified image of the sky is projected on the chip on the back surface of the elliptical lens (L6).

In SIR configuration there is no optical component for inserting an LO beam, since the LO is integrated on the receiver chip, where suitable planar components provide coupling to the SIS detector.

Table 1. Parameters of the integrated lens-antenna calculated by PILRAP at 625 GHz.

Lens diameter, mm	10
Lens material	Silicon, ε_r=11.7
Gaussian beam efficiency, %	92.7
Minimum beam waist, mm	3.8
-3dB beamwidth, deg	3
-10dB beamwidth, deg	5.3
Sidelobes level, dB	-20
Spillover efficiency, %	87.7
Directivity, dBi	35

2.3 Quasioptical performance of the cold channel

The quasioptical performance of the cold channel is modelled using fundamental mode Gaussian beam calculations at 625 GHz. The off-axis curved mirrors are represented by classical thin lenses, while the input beam is modelled as a fundamental Gaussian with a λ-independent waist located 160 mm in front of L1. This simple approach ignores any non-ideal effects in the system.

In the Fig. 5 we show both, the optical and quasi-optical trajectories (radii in mm) between the optical components. This assumes a single fundamental Gaussian mode only.

The trajectories are dotted lines (optical) and continuous lines (quasi-optical). The curved mirrors, the window and the integrated lens-antenna are schematically given as thin vertical lines, representing thin lenses. Also indicated is the position and size of the SSB filter envelope. Note that the vertical scale is very different from the horizontal one.

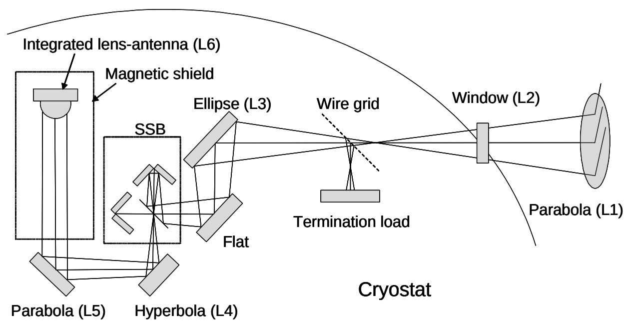

Fig. 4. Layout of the cold channel optics. Lines show the optical beam trajectories.

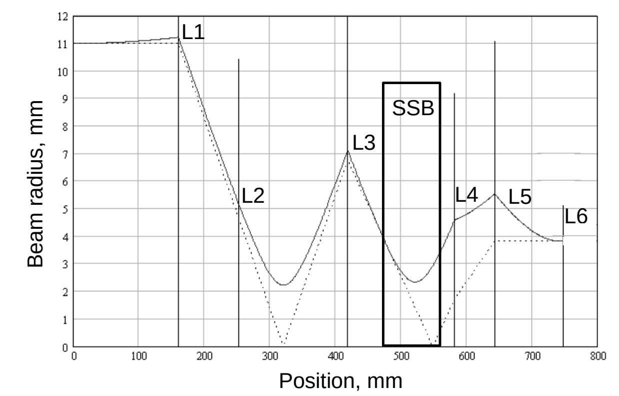

Fig. 5. Optical (dotted line) and quasioptical (solid line) trajectories (1/e field level) in the cold channel. The curved mirrors (L1), (L3), (L4) and L5), the window (L2) and the integrated lens-antenna (L6) are given schematically as thin vertical lines, representing thin lenses.

All optical components have a minimum diameter of 4 beam radii (1/e field level), corresponding to an edge taper of -35 dB. Only the integrated lens is smaller than 4 beam radii. (L3), (L4) and (L5) mirrors are √2 larger in horizontal direction than in vertical direction, because of the 45 degrees angle of incidence.

3 VERIFICATION OF THE OPTICAL DESIGN

Simulation of reflective optics with fundamental Gaussian beam analysis is in general not very accurate. When using off-axis parabolic mirrors, the initial circularly symmetric beam becomes weighted towards one side because of the difference in path lengths to the two edges of the mirror in the plane of incidence. Also, if the reflective mirror is in the near field region, then the analysis based on geometrical optics is not accurate enough. Only analysis based on the Physical Optics (PO) could be used to study in full the effects of asymmetry.

The quasi-optical performance of the reflective optics of the TELIS instrument has been calculated using the GRASP8 package (from TICRA in Denmark). GRASP8 is a set of tools for analyzing general reflector antennas and antenna farms that is based upon well established PO analysis techniques, supplemented where appropriate with the Physical Theory of Diffraction, Geometrical Optics, and Uniform Geometrical Theory of Diffraction. GRASP8 (and its predecessor, GRASP7) has been widely used in industry for many years, and many comparisons of its results with real measurements have been reported in scientific and engineering literature.

Detailed GRASP analysis of the TELIS optics and in particular of the telescope is reported in the paper by A. Murk et al, of this Proceedings [2].

To simulate the 550-650 GHz cold channel we used configuration illustrated by Fig. 4. The center frequency is 625 GHz. As an input feed, the calculated by PILRAP integrated lens-antenna system field distribution is used. The SSB filter is replaced by a set of two plane mirrors as we could not find a way to model accurately roof top mirrors in GRASP.

Fig. 6 shows the far field beam profile simulated by GRASP. Solid lines are the power patterns in the vertical (perpendicular to the optics base plate) and horizontal planes. One can see that in one plane (vertical) the beam is absolutely symmetric. A 13% asymmetry (expressed as a difference of integrated powers in positive and negative angles) in the horizontal plane is caused by non-axissymmetric optics in this plane. The dotted line indicates a cross-polarization component which appears at <-20 dB level. Just for a reference purpose, an ideal Gaussian beam profile is indicated by dashed line.

Complete optics of the 550-650 GHz receiver, including the cold channel, warm optics and the telescope (as drawn in Fig. 1), was also simulated by GRASP. Fig. 7 shows calculated 2-D far field pattern of the receiver at 625 GHz. The pattern exhibits an elliptical form (note different scale in azimuth and elevation) determined by the anamorphicity of the telescope. Strongly asymmetric pattern in the azimuth plane is mainly caused by the fast off-axis optics of the telescope. However, for the atmospheric limb scans, only the vertical (elevation) profile of the receiver beam is of interest for the retrieval, while the atmosphere is uniform in the horizontal plane within the field of view. The 2-D results were used to calculate the 1-D vertical profile and Azimuthally Collapsed Antenna Pattern (ACAP) by summing over the co- and cross-polarization amplitudes at each elevation, Fig. 8. FWHM of the ACAP at 625 GHz is 0.17 deg, corresponding to a 1.65 km FWHM beam at the tangent point in 550 km distance. The ACAP is

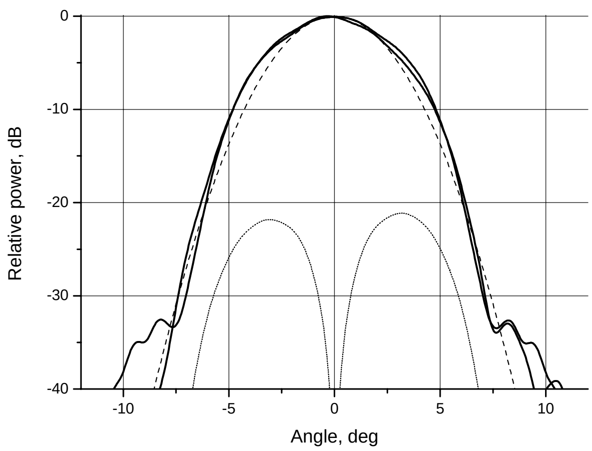

Fig. 6. Calculated far field beam pattern of the 550-650 GHz cold channel. Frequency is 625 GHz. Solid lines show beam pattern in two orthogonal planes. Dotted line is a cross-polarization component. An ideal Gaussian profile is indicated by the dashed line.

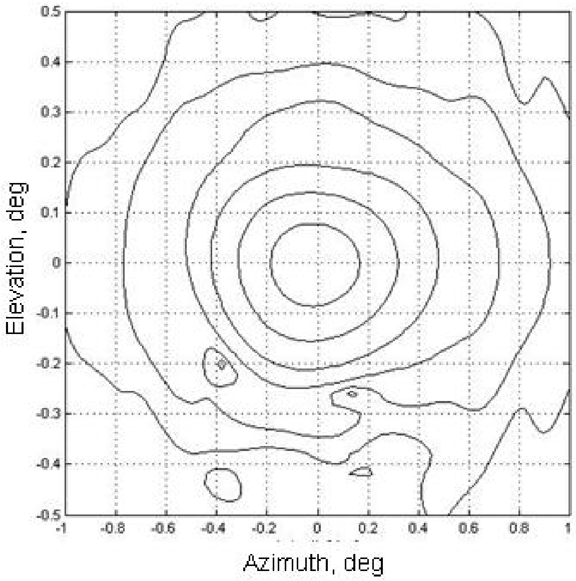

Fig. 7. Calculated far field 2-D beam profile of the 550-650 GHz instrument at 625 GHz. Solid lines represent the -3 dB and the -10 dB to -50 dB contours.

symmetric and has an almost Gaussian shape for amplitudes larger than -20 dB. An symmetric sidelobe starts at the -25 dB level. This beam shape will be relevant for the retrieval of atmospheric data and has to be considered in the retrieval model. The calculated total spillover loss of the optics (not including the integrated lens-antenna) is 5%.

4 ALIGNMENT PLAN AND TOLERANCES

An optical configuration of the TELIS SIR channel consists of about 20 optical elements, located within three major sub-assemblies: telescope, warm optics and cold channel. Fabrication and positioning errors of each element and sub-assemblies as a whole cause deviation of the optical performance from the ideal design. Therefore, comprehensive study of mechanical tolerances and their impact on the system performance

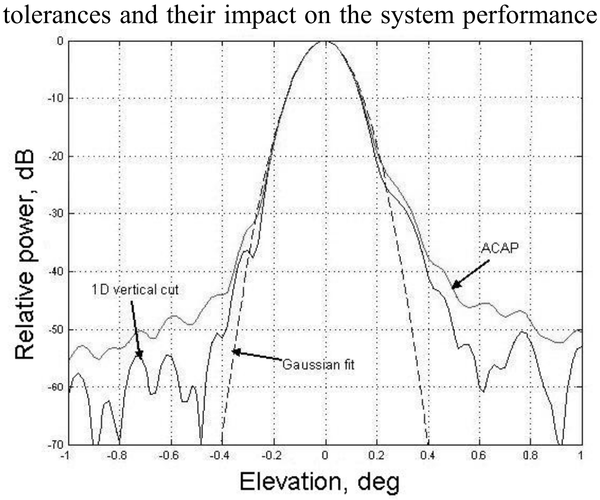

Fig. 8. Calculated far field 1-D vertical (elevation) cut and ACAP at 625 GHz.

has been performed using commercial programs ZEMAX for Geometrical Optics analysis and GRASP for Physical Optics analysis.

There are other factors as well which cause deterioration of the system performance during the maintenance. These are thermal effects, position non-reproducibility of the sub-assemblies or potential deformations caused by 5g acceleration during instrument landing. These all made it absolutely necessary to envisage visible light alignment and/or verification. For this reason, all reflective optical elements, including the telescope, are required to have an optical surface quality.

4.1 Geometrical optics analysis

As a first step, an inverse sensitivity analysis of mechanical tolerances was performed. Both linear and angular misalignments of each optical element were considered. Shapes of reflecting surfaces were assumed to be ideal. In the inverse sensitivity mode ZEMAX computes the value of each tolerance that will result in the decrease in performance specified by Max Criteria. Only one optical element is perturbed at once, other elements remain unperturbed. For the Max Criteria we selected a maximum offset of 1/3 beam radius (1/e field level) at each mirror. This criterion keeps under control the aperture efficiency and spillover loss as the size of all optical elements is 4 beam radii. Calculations are performed iteratively inside a loop while adjustments are made to the min and max tolerances to meet the Max Criterion specs. This analysis identifies optical elements most critical to the misalignments and their individual tolerances.

As a next step, statistical (Monte Carlo) analysis of the tolerances was performed. This method analyses the effect of all perturbations simultaneously. For each Monte Carlo cycle, all parameters which have specified tolerances are randomly set using the defined range of the parameter (found by the inverse sensitivity analysis) and a statistical model of the distribution of that parameter over the specified range. By default, all parameters are assumed to follow the same normal distribution with a total width of four standard deviations between the extreme minimum and maximum allowed values. More than 200 Monte Carlo cycles were run to get statistics on performance degradation.

As a last step, all tolerances, and especially those of most critical mirrors, have been tightened until the performance degradation is in 90% of the runs within the Max Criteria mentioned above.

Similar analysis was performed for the groups of elements. This covers the cases of global misalignment of the cold channel and the telescope with respect to the warm optics.

The geometrical optics tolerance analysis allowed us to draw the following conclusions:

1. There are two mirrors in the cold channel with an angular tolerance of 0.06-0.08 deg. This can be

translated to a linear tolerance of about 20 micrometers, feasible with CNC machining.
2. All elements of the cold channel can be mounted on the common baseplate using dead-reckoning, if the above mentioned mechanical accuracy is maintained for all mirrors and the baseplate. Visible light alignment verification should be performed to check for fabrication errors.
3. Position accuracy of the chip on the lens should be better than 10 micrometers.
4. Within the warm optics, the typical angular tolerances are 0.1-0.2 deg, translated to about 30 micrometers requirements for the production.
5. The telescope should be aligned with visible light.
6. The tolerances on position and rotation of groups of elements can not be met. For example, the absolute position of the cold channel mount plate inside the crystat is not better than 0.5 mm. Moreover, this position may not be reproducible between the cryostat cooling. Therefore, two first (after the telescope) and last mirrors in the warm optics should have alignment possibility to (co)align the warm optics with the telescope and cold channel, respectively.

4.2 Physical Optics analysis

The physical optics simulations are time consuming and allow only a limited number of cases to be analyzed. We have selected the cases of global misalignments between the sub-assemblies.
The simulations of the telescope to warm optics misalignments showed that ±1 mm lateral and ±0.5 deg misalignments do not degrade substantially the quality of the beam, and keep it within the requirements. The FWHM of the ACAP changes are within 3%, spillover loss is not increased by more than 0.5%, the difference in sidelobes is only noticeable at <-25 dB level. A maximum pointing error of ±0.04 deg will cause a beam shift of ±0.4 km at the tangent point, close to the requirement on ±0.5 km beams co-alignment on the sky of the three frequency channels of TELIS instrument.
A case of warm optics to cold channel misalignments is particularly interesting as the reproducibility of the cold channel mount in the cryostat is not yet known and could be poor because of thermal cycling. In this case, the effects of lateral misalignments of ±1 mm and angular misalignments of ±0.3 deg were investigated. Here, the results are in general very similar to the previous case. Note only that here the angular tolerances are almost a factor of two tighter. For the illustration how the beam is affected by the misalignments, the three beam profiles are shown in the Fig. 9. One (solid line) shows the ACAP of the ideal (aligned) case. The other two curves (dashed and dotted lines) are the beam resulted from the 1 mm

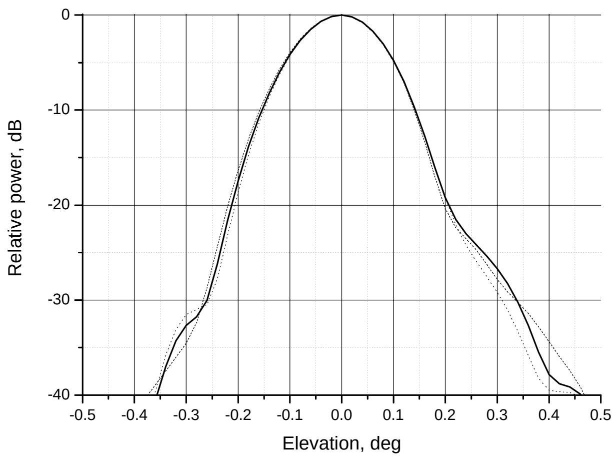

Fig. 9. ACAP of the 550-650 GHz channel beam for the three cases of warm optics to cold channel misalignment. Solid line shows the ACAP of the ideal case. The other two curves (dashed and dotted lines) are the beam resulted from the 1 mm lateral misalignments of the cold box in the planes perpendicular to the beam.

lateral misalignments of the cold box in the planes perpendicular to the beam. The FWHM of ACAP change is within 2%, the maximum spillover loss change is 1%, the difference in sidelobes is noticeable at <-20 dB level. The pointing error in this case is larger, about 0.07 deg, corresponding to 0.7 km pointing offset at the tangent point. Note, that the pointing offsets are corrected in the data presented in the Fig. 9. Similar results are for the angular misalignments of ±0.3 deg.
In conclusion, we have shown that the main requirements on the maximum performance degradation due to sub-assemblies misalignments could be met if the tolerances are within ±1 mm and ±0.5 deg for the telescope-warm optics interface and ±1 mm and ±0.3 deg for the cold channel-warm optics interface. Only the pointing error is slightly outside the specs. Note, however, that due to PO computational time limitations, the sensitivity analysis was restricted by the cases when only one interface between three sub-assemblies is perturbed, the other one stayed perfect. Therefore, the tolerances estimated here can only be used as a guideline.

ACKNOWLEDGEMENTS

The work was supported in parts by the RFBR projects 03-02-16748, INTAS project 01-0367, ISTC projects # 2445, 3174 and the President Grant for the Scientific School 1344.2003.2.
The authors thank M. van der Vorst for supplying PILRAP (Program for Integrated Lens and Reflector Antenna Parameters). T. de Graauw, A. Selig and W. Wild are acknowledged for their support in this work, G. Wagner and N. Whyborn for useful and stimulating discussions.

REFERENCES

1. Hoogeveen, R.W.M., Yagoubov, P.A., Maurellis, A.N., Koshelets, V.P., Shitov, S.V., Mair, U., Krocka, M., Wagner, G., Birk, M., Hübers, H.-W., Richter, H., Semenov, A., Gol`tsman, G., Voronov, B., Ellison, B., Kerridge, B., Matheson, D., Alderman, B., Harman, M., Siddans, R., Reburn, J., eds. Strojnik, M., “New cryogenic heterodyne techniques applied in TELIS: the balloon borne THz and submm limb sounder for atmospheric research”, Proc. of SPIE, Infrared Spaceborne Remote Sensing XI, 5152, p. 347-355, 2004.
2. A. Murk, P. Yagoubov, U. Mair, M. Birk, G. Wagner, H. van de Stadt, R. Hoogeveen, N. Kampfer, “Antenna simulations for the THz and submm limb sounder TELIS”, in this Conference Proceedings.
3. Koshelets, V.P., Shitov, S.V., Filippenko, L.V., Dmitriev, P.N., Ermakov, A.B., Sobolev, A.S., Torgashin, M.Y., Pankratov, A.L., Kurin, V.V., Yagoubov, P., Hoogeveen, R., “A superconducting phase-locked local oscillator for a submillimeter integrated receiver”, Supercond. Sci. Technol., 17, p. S127-S131, 2004.
4. V.P. Koshelets, S.V. Shitov, A.B. Ermakov, O.V. Koryukin, L.V. Filippenko, A.V. Khudchenko, M.Yu. Torgashin, P. Yagoubov, R. Hoogeveen, O.M. Pylypenko, "Superconducting Integrated Receiver for TELIS", Applied Superconductivity Conference ASC'2004, USA, October, 2004; Report 2ET06; "IEEE Trans. on Appl. Supercond.", vol. 15, 2005.
5. D.F.Filipovic, S.S.Gearhart, and G.M.Rebeiz, "Double-slot antennas on extended hemispherical and elliptical silicon dielectric lenses," IEEE Trans. Microwave Theory Tech., vol. 41, pp. 1738-1749, 1993.
6. D.H. Martin and E. Pupplet, *Infrared Phys.*, vol. 10, pp. 105–109, 1969.
7. P. Goldsmith, “Quasioptical Systems: Gaussian Beam Quasioptical Propagation and Applications”, IEEE Press Series on RF and Microwave Technology, Series Editors: Roger D. Pollard and Richard Booton.